MOLECULAR AND CELLULAR BIOLOGY, Nov. 2010, p. 5207–5217 Vol. 30, No. 21
0270-7306/10/$12.00 doi:10.1128/MCB.00366-10

The Function of Two Rho Family GTPases Is Determined by Distinct Patterns of Cell Surface Localization▽

Hao Wu and Patrick Brennwald*

Department of Cell and Developmental Biology, University of North Carolina at Chapel Hill, Chapel Hill, North Carolina 27599-7090

Received 29 March 2010/Returned for modification 24 May 2010/Accepted 25 August 2010

Rho family GTPases are critical regulators in determining and maintaining cell polarity. In *Saccharomyces cerevisiae*, Rho3 and Cdc42 play important but distinct roles in regulating polarized exocytosis and overall polarity. Cdc42 is highly polarized during bud emergence and is specifically required for exocytosis at this stage. In contrast, Rho3 appears to play an important role during the isotropic growth of larger buds. Using a novel monoclonal antibody against Rho3, we find that Rho3 localizes to the cell surface in a dispersed pattern which is clearly distinct from that of Cdc42. Using chimeric forms of these GTPases, we demonstrate that a small region at the N terminus is necessary and sufficient to confer Rho3 localization and function onto Cdc42. Analysis of this domain reveals two essential elements responsible for distinguishing function. First, palmitoylation of a cysteine residue by the Akr1 palmitoyltransferase is required both for the switch of function and the switch of localization properties of this domain. Second, two basic residues distal to the palmitoylation site are required for regulating binding affinity with the Exo70 and Sec3 effectors. This demonstrates the importance of localization and effector binding in determining how these GTPases evolved specific functions at distinct stages of polarized growth.

Cell polarity is a highly conserved feature of eukaryotic cells and is important for a number of events in animal cell biology, including embryonic development, cell migration, and epithelial function (21). The budding yeast *Saccharomyces cerevisiae* provides a simple model system in which to understand cell polarity, as much of the machinery that is responsible for polarity between yeast and animal cells is highly conserved. Rho/Cdc42 family GTPases are examples of this conservation and have been shown to be critical determinants of polarity in both yeast and animal cells. Rho GTPases are thought to exert their effects on cell polarization through regulation of a number of cellular processes, including the cytoskeleton and polarized delivery of new membrane to sites of active growth.

Previous studies have demonstrated that Rho3 and Cdc42 have direct roles in regulating exocytosis which are independent of their role in regulating the polarity of the actin cytoskeleton (1, 2). Studies from a number of laboratories have shown that a multisubunit vesicle tethering complex known as the exocyst is likely to be a critical effector for Rho/Cdc42 signaling during polarized exocytosis (1, 2, 11, 22). A number of models have been suggested to describe the action of Rho GTPases in regulating exocytic function (28, 30). Analysis of specific loss-of-function alleles of *RHO3* and *CDC42* demonstrated that defects in secretion could be distinguished not only from actin polarity but from the polarization of the exocytic machinery as well. This led to the suggestion that Rho GTPases act by local activation rather than recruitment of the exocytic machinery (25).

Genetic analysis suggests that the pathway by which Cdc42 regulates secretion is closely linked to that of Rho3. Secretion-defective alleles in each of these GTPases are suppressed by a common set of genes, and the mutants exhibit synthetic lethality when combined in the same cell (1). Recent work has provided direct evidence that the Exo70 subunit of the exocyst both genetically and physically interacts with both Rho3 and Cdc42 (29).

Although Rho3 and Cdc42 share a effector and have overlapping functions, there are different characteristics in how these two proteins regulate exocytosis in yeast. Analysis of the Rho3 and Cdc42 secretory mutants by electron microscopy and secretory assays revealed that *cdc42-6* mutants showed defects only in cells with small or emerging buds; in contrast, *rho3-V51* mutants exhibited secretory defects throughout bud growth (1, 2). These phenotypes suggested that the exocytic function of Rho3 and Cdc42 is required at overlapping but distinct stages of bud growth.

Most small GTPases require multiple elements to promote their association with the membrane on which they engage their downstream targets (26). Modification of the C-terminal CAAX motif by prenylation is common to both Rho3 and Cdc42, with Rho3 predicted to be farnesylated and Cdc42 shown to be geranylgeranylated (14, 17, 19). However, as with other small GTPases, C-terminal prenylation by itself is not sufficient for stable membrane association (10, 18). As with many other small GTPases, a second site of interaction is thought to be required for both Rho3 and Cdc42 GTPases. Sequence alignment of Rho3 and Cdc42 revealed that Rho3 has a long N-terminal extension, which contains a site (a cysteine at position 5) for palmitoylation (24). In contrast, Cdc42 is not palmitoylated but instead contains a polybasic domain adjacent to the CAAX motif at its C terminus, which is thought to act as a membrane targeting signal via the electrostatic interactions with phospholipids at the plasma membrane (6, 12).

* Corresponding author. Mailing address: Department of Cell and Developmental Biology, University of North Carolina at Chapel Hill, 522 Taylor Hall, CB#7090, Chapel Hill, NC 27599-7090. Phone: (919) 843-4995. Fax: (919) 966-1856. E-mail: pjbrennw@med.unc.edu.

▽ Published ahead of print on 7 September 2010.

TABLE 1. Yeast strains used in this study

Strain	Genotype	Reference
BY1426	*MAT***a** *rho3*Δ::*LEU2 ura3-52 his3-*Δ*200 leu2-3,112* pRS316 *RHO3*	P. Brennwald collection
BY1595	*MAT***a** *rho3*Δ::*LEU2 ura3-52 his3-*Δ*200 leu2-3,112* pRS313 *RHO3*	This study
BY1689	*MAT***a** *rho3*Δ::*LEU2 leu2-3,112 ura3-52 his3-*Δ*200* pRS313 *RHO3C5A*	This study
BY1718	*MAT***a** *rho3*Δ::*LEU2 leu2-3,112 ura3-52 his3-*Δ*200* pRS313 *RHO3A3,4*	This study
BY1807	*MAT***a** *cdc42*Δ::*HIS3 ura3-52 leu2-3,112* pRS316 *CDC42*	P. Brennwald collection
BY1846	*MAT***a** *cdc42*Δ::*HIS3 ura3-52 his3-*Δ*200 leu2-3,112* pRS315 *CDC42NT^{R3}A3,4*	This study
BY2101	*MAT***a** *rho3*Δ::*LEU2 akr1*Δ::*KanMX6 ura3-52 his3-*Δ*200 leu2-3,112* pRS316 *RHO3*	This study
BY2102	*MAT***a** *rho3*Δ::*LEU2 erf2*Δ::*KanMX6 ura3-52 his3-*Δ*200 leu2-3,112* pRS316 *RHO3*	This study
BY2103	*MAT***a** *rho3*Δ::*LEU2 pfa4*Δ::*KanMX6 ura3-52 his3-*Δ*200 leu2-3,112* pRS316 *RHO3*	This study
BY2119	*MAT***a** *rho3*Δ::*LEU2 akr2*Δ::*KanMX6 ura3-52 his3-*Δ*200 leu2-3,112* pRS316 *RHO3*	This study
BY2120	*MAT***a** *rho3*Δ::*LEU2 swf1*Δ::*KanMX6 ura3-52 his3-*Δ*200 leu2-3,112* pRS316 *RHO3*	This study
BY2121	*MAT***a** *rho3*Δ::*LEU2 pfa3*Δ::*KanMX6 ura3-52 his3-*Δ*200 leu2-3,112* pRS316 *RHO3*	This study
BY2122	*MAT***a** *rho3*Δ::*LEU2 pfa5*Δ::*KanMX6 ura3-52 his3-*Δ*200 leu2-3,112* pRS316 *RHO3*	This study
BY2123	*MAT***a** *cdc42*Δ::*HIS3 akr1*Δ::*KanMX6 trp1-*Δ*63 ura3-52 his3-*Δ*200 leu2-*Δ *lys2-801* pRS316 *CDC42*	This study
BY2124	*MAT***a** *cdc42*Δ::*HIS3 akr2*Δ::*KanMX6 trp1-*Δ*63 ura3-52 his3-*Δ*200 leu2-*Δ *lys2-801* pRS316 *CDC42*	This study
BY2125	*MAT***a** *cdc42*Δ::*HIS3 erf2*Δ::*KanMX6 trp1-*Δ*63 ura3-52 his3-*Δ*200 leu2-*Δ *lys2-801* pRS316 *CDC42*	This study
BY2126	*MAT***a** *cdc42*Δ::*HIS3 swf1*Δ::*KanMX6 trp1-*Δ*63 ura3-52 his3-*Δ*200 leu2-*Δ *lys2-801* pRS316 *CDC42*	This study
BY2127	*MAT***a** *cdc42*Δ::*HIS3 pfa3*Δ::*KanMX6 trp1-*Δ*63 ura3-52 his3-*Δ*200 leu2-*Δ *lys2-801* pRS316 *CDC42*	This study
BY2128	*MAT***a** *cdc42*Δ::*HIS3 pfa4*Δ::*KanMX6 trp1-*Δ*63 ura3-52 his3-*Δ*200 leu2-*Δ *lys2-801* pRS316 *CDC42*	This study
BY2129	*MAT***a** *cdc42*Δ::*HIS3 pfa5*Δ::*KanMX6 trp1-*Δ*63 ura3-52 his3-*Δ*200 leu2-*Δ *lys2-801* pRS316 *CDC42*	This study
BY2232	*MAT***a** *cdc42*Δ::*HIS3 ura3-52 his3-*Δ*200 leu2-3,112* pRS315 *CDC42-NT^{Rho3}A17,18*	This study
BY2233	*MAT***a** *cdc42*Δ::*HIS3 ura3-52 his3-*Δ*200 leu2-3,112* pRS315 *CDC42-NT^{Rho3C5A}*	This study
BY2234	*MAT***a** *cdc42*Δ::*HIS3 ura3-52 his3-*Δ*200 leu2-3,112* pRS315 *CDC42-NT^{Rho3}*	This study
BY2236	*MAT***a** *cdc42*Δ::*HIS3 ura3-52 his3-*Δ*200 leu2-3,112* pRS315 *CDC42*	This study
BY2486	*MAT***a** *rho3*Δ::*LEU2 ura3-52 his3-*Δ*200 leu2-3,112* pRS316 *rho3-NT^{C42}* pRS313 *CDC42-NT^{R3}*	This study
BY2487	*MAT***a** *rho3*Δ::*LEU2 ura3-52 his3-*Δ*200 leu2-3,112* pRS316 *rho3-A17,18* pRS313 *CDC42-NT^{R3}*	This study

In this study we examine how the function and localization of two Rho GTPases are specified at distinct stages of polarized growth in yeast. Using a novel monoclonal antibody, we find that the pattern of cell surface localization observed for the Rho3 GTPase is clearly distinct from that of Cdc42. Using chimeric forms of these GTPases, we find that the N terminus plays a particularly important role in this specification. The functional effect imparted by the N terminus appears to have two key elements. One element involves palmitoylation of a cysteine in the N terminus of Rho3 that is critical in generating the dispersed pattern of localization observed for Rho3. A second element regulates the affinity of the GTPases for a common effector, the exocyst complex. Taken together, this work provides a model for how these GTPases have evolved distinct functions by adopting sequence elements that affect both the pattern of localization and the ability to engage the downstream effector in a way that allows each GTPase to function at different stages of polarized growth.

MATERIALS AND METHODS

Yeast strains, reagents, and genetic techniques. Yeast strains used in this study are listed in Table 1. Standard methods were used for yeast media and genetic manipulations. Cells were grown in YPD medium containing 1% Bacto-yeast extract, 2% Bacto-peptone, and 2% glucose. The components of the medium were from Fisher Scientific. Sorbitol, sodium azide (NaN_3), sodium fluoride (NaF), ethanolamine, β-mercaptoethanol, Triton X-100, and HIS-select nickel affinity gel were obtained from Sigma Chemical (St. Louis, MO). Zymolyase (100T) was from Seikagaku (Tokyo, Japan). Tween 20 (10%) was from Bio-Rad. Dithiothreitol (DTT), bovine serum albumin (BSA), yeast nitrogen base, raffinose, galactose, and 5-fluoroorotic acid (5-FOA) were from US Biologicals (Swampscott, MA). Glutathione-Sepharose beads were from Amersham Biosciences. Secondary antibodies for the Odyssey Imaging system were from LI-COR Biosciences and Molecular Probes. Secondary antibodies for immunofluorescence were from Jackson ImmunoResearch. Formaldehyde (37%) was from Electron Microscopy Sciences (Ft. Washington, PA). FluorSave reagent (mounting medium) was from Calbiochem. Slides for immunofluorescence were from Carlson Scientific, Inc. The bead beater for making yeast lysate was from Biospec Products. Transformations for suppression analysis were performed using the lithium acetate method described by Guthrie and Fink (9).

Plasmid construction. Plasmids used in this study are listed in Table 2. pB1366

TABLE 2. Plasmids used in this study

Strain	Host	Plasmid description
BB442	BL21	pGEX4T1 *SEC9* (aa 402 to 651)
BB1366	DH5α	pRS313 *RHO3*
BB1367	DH5α	pRS313 *CDC42*
BB1368	DH5α	pRS313 *rho3-NT^{C42}*
BB1516	XL1-Blue	pRS313 *RHO3-Q2*
BB1590	DH5α	pRS313 *RHO3-A3,4*
BB1515	XL1-Blue	pRS313 *RHO3-A5*
BB1521	DH5α	pRS313 *rho3-A7-11*
BB1592	DH5α	pRS313 *RHO3-A12-15*
BB1591	DH5α	pRS313 *rho3-A16-19*
BB1691	DH5α	pRS313 *rho3-A17,18*
BB1369	DH5α	pRS313 *CDC42-NT^{R3}*
BB1483	DH5α	pRS315 *CDC42-NT^{R3}*
BB1522	DH5α	pRS313 *CDC42-NT^{R3}Q2*
BB1523	DH5α	pRS313 *CDC42-NT^{R3}A5*
BB1524	DH5α	pRS313 *CDC42-NT^{R3}A7-11*
BB1532	DH5α	pRS315 *CDC42-NT^{R3}Q2*
BB1533	DH5α	pRS315 *CDC42-NT^{R3}A5*
BB1534	DH5α	pRS315 *CDC42-NT^{R3}A7-11*
BB1587	BL21	pGEX6P1PH *EXO70*
BB1588	DH5α	pRS313 *CDC42-NT^{R3}A16-19*
BB1589	DH5α	pRS313 *CDC42-NT^{R3}A12-15*
BB1593	DH5α	pRS315 *CDC42-NT^{R3}A12-15*
BB1594	DH5α	pRS313 *CDC42-NT^{R3}A3,4*
BB1596	DH5α	pRS315 *CDC42-NT^{R3}A3,4*
BB1597	DH5α	pRS315 *CDC42-NT^{R3}A16-19*
BB1598	DH5α	pRS313 *CDC42-NT^{R3}A17,18*
BB1731	DH5α	pRS315 *CDC42*
BB1857	DH5α	pRS315 *CDC42-NT^{R3}A6*
BB1964	DH5α	pRS316 *rho3-A17,18*

(pRS313 *RHO3*) and pB1367(pRS313 *CDC42*) were generated by subcloning a BglII and SalI fragment containing the entire open reading frame of *RHO3* and *CDC42* as well as the 500-bp promoter region and 250-bp 5′ untranslated region (UTR) into the pRS313 vector. The resulting plasmids were then used as the backbone for creating the *RHO3-CDC42* chimera. Chimeric genes *CDC42-NT^{R3}* and *rho3-NT^{C42}* were constructed by overlapping PCRs and verified by DNA sequencing (13, 31).

Protein purification and quantification. The pGEX-6P6H (pB1579) plasmid was constructed as described previously (29). This vector was used to create the following glutathione *S*-transferase (GST) fusion constructs: GST-Sec3 (amino acids [aa] 1 to 319) and GST-Exo70 (aa 1 to 623). All constructs were confirmed by sequencing, and protein expression was performed with *Escherichia coli* BL21 cells. Cells were grown at 37°C in terrific broth medium to an optical density at 599 nm (OD_{599}) of 2.0 to 2.5. Cells were shifted to 25°C, and protein expression was induced with 0.1 mM IPTG (isopropyl-β-D-thiogalactopyranoside) for 3 h at 25°C.

6×His tag purification was performed by binding the bacterial lysate to HIS-select nickel affinity gel (Sigma), followed by eluting the GST fusion proteins with 500 mM imidazole. The 6×His eluates were then incubated with glutathione-Sepharose beads at 4°C for 1 h and then washed with wash buffer (20 mM Tris, pH 7.5, 120 mM NaCl, and 1% Tween 20) to remove unbound proteins. Protein concentration was determined by comparison to purified protein standards after SDS-PAGE and Coomassie blue staining. Quantification of Coomassie blue-stained gels was performed with an Odyssey infrared imaging system (LiCor).

Generation of yeast cell lysates. *RHO3L74*, *rho3-NT^{C42}L61*, *rho3-L74A17,18 CDC42-L61*, and *CDC42-NT^{R3}L74* were amplified by PCR and subcloned behind the *GAL1* promoter in a *LEU2* integrating vector (BB24, pRS305 with *GAL1* promoter). The vector was linearized by digesting with BstXI and transformed into a wild-type Gal$^+$ strain, BY17 (**a** *GAL1 leu2-3,112 ura3-52*). Yeast strains were grown overnight in YP with 3% raffinose at 30°C to mid-log phase with an OD_{599} of 1 to 1.5 and then induced with 1% galactose for 4 h at 30°C. Cells were pelleted by centrifugation at 5,000 rpm for 5 min and washed with double-distilled water (ddH_2O). Pellets were immediately frozen on dry ice. Frozen pellets were lysed with lysis buffer using a bead beater from Biospec Products. The optimal wet weight for the small chamber was 5 to 6 g. The pellet was beaten for 1 min followed by a 3-min pause for five cycles. The resulting lysate was then subjected to centrifugation for 10 min at 17,000 × *g*, followed by ultracentrifugation at 100,000 × *g* for 30 min. The protein concentration of the lysate was measured by a Bradford assay. Each lysate was normalized to about 25 mg/ml total protein concentration and frozen on dry ice.

GST pulldown from yeast cell lysates. All recombinant proteins were present at a final concentration of 3 μM. Cell lysates for GST pulldown experiments were prepared as described above and incubated with each fusion protein on glutathione-Sepharose beads for 1.5 h at 4°C. The beads were washed five times with lysis buffer (20 mM Tris-HCl, pH 7.5, 120 mM NaCl, 10 mM $MgCl_2$, 1% Tween 20, 1 mM DTT) and boiled at 95°C for 5 min. Samples were subjected to SDS-PAGE analysis and blotted with Rho3 and Cdc42 monoclonal antibodies. Quantification of Western blots was performed with an Odyssey infrared imaging system.

Antibodies. Monoclonal antibodies raised against GST-Rho3 and GST-Cdc42 were isolated and production cell culture supernatants generated in collaboration with the University of North Carolina (UNC) Immunology Core facility. Generation of affinity-purified rabbit polyclonal antibodies against Cdc42 was described previously (1).

Immunofluorescence. Cells were grown overnight to mid-log phase and fixed immediately with 37% formaldehyde. Fixed cells were spheroplasted, permeabilized with 0.5% SDS, and affixed to the slides as described previously (5, 25). Immunostaining was performed using a mouse monoclonal antibody against Rho3 (monoclonal antibody [MAb] 4-51) at a 1:5 to 1:50 dilution of cell culture supernatant and an affinity-purified rabbit polyclonal antibody against Cdc42 at a 1:75 dilution. The mouse monoclonal antibody against Cdc42 (MAb28-10) was used for immunofluorescence at a 1:25 to 1:50 dilution of cell culture supernatant. Rhodamine Red-X-AffiniPure goat anti-mouse IgG and fluorescein isothiocyanate (FITC)-conjugated goat anti-rabbit IgG (Jackson ImmunoResearch Laboratories, West Grove, PA) were used at a 1:50 dilution for detection of Rho3 and Cdc42, respectively. Stained cells were viewed using a microscope (model E600; Nikon) equipped with a 512- by 512-pixel back-illuminated frame transfer charge-coupled-device camera (Princeton Instruments) and Metamorph software (Universal Imaging Corp.). Approximately 200 cells were randomly selected for quantitation. Small-budded cells were defined as cells with buds smaller than half the size of the mother cell, and large-budded cells were defined as cells with buds larger than half the size of the mother cell.

Subcellular fractionation. Wild-type cells containing *rho3-NTC42*, *RHO3-A3,4*, *RHO3-A5*, and *rho3-A17,18* (see Fig. 3E) or palmitoyltransferase deletion strains containing wild-type *RHO3* (see Fig. 5C) were grown overnight in selective media, harvested, and grown in rich medium for 2 h. Yeast cells (approximately 200 OD_{599} units) were washed with 10/20/20 buffer (10 mM Tris, pH 7.5, 20 mM NaN_3, and 20 mM NaF) and spheroplasted in 7.2 ml of spheroplast buffer (0.1 M Tris, 10 mM azide, 1.2 M sorbitol, and 21 mM β-mercaptoethanol with 0.08 mg/ml Zymolyase 100T) for 30 min at 37°C. The spheroplasts were lysed in 5 ml of ice-cold triethanolamine (TEA)-sorbitol (10 mM TEA, pH 7.2, and 0.8 M sorbitol) with a protease inhibitor cocktail [1 mg/ml each of leupeptin, aprotinin, antipain, 0.5 mM phenylmethylsulfonyl fluoride (PMSF), 20 mM pepstatin A, and 2 mM 4-(2-aminoethyl)benzenesulfonyl fluoride] and spun at 450 × *g* for 3 min in a cold centrifuge to remove unbroken cells. The lysates were spun at 30,000 × *g* for 20 min at 4°C in a Sorvall centrifuge tube to separate the supernatant and pellet fractions. All pellets were normalized to the volume of the supernatant fractions. Equal volumes of total lysate and supernatant and pellet fractions were boiled in SDS sample buffer, run on a 15% SDS-polyacrylamide gel, and blotted with polyclonal Sso1/2 antibody (1:2,000), monoclonal Rho3 antibody (1:200), or Cdc42 antibody (1:250). Quantification of Western blots was performed with an Odyssey infrared imaging system.

RESULTS

Rho3 and Cdc42 have distinct localization patterns on the plasma membrane. The function of Cdc42 in polarized growth is thought to be closely tied to its highly polarized pattern of localization on the plasma membrane. Consistent with this notion, we have previously shown that Cdc42 mutants defective in exocytic function demonstrate this defect only during early bud emergence, when the localization of Cdc42 is highly polarized, and not at later stages of bud growth. In contrast, secretion-defective mutants in the Rho3 GTPase demonstrate defects throughout bud growth. However, the intracellular localization of Rho3 at endogenous levels of expression has not been described (see Discussion). We have isolated a new monoclonal antibody to Rho3, which we have used in double-labeling experiments to examine the pattern of localization compared to that of Cdc42. The results, shown in Fig. 1, demonstrate a surprisingly distinct staining pattern for Rho3. In stark contrast to the tightly polarized localization of Cdc42, Rho3 localizes along most of the plasma membrane and is only slightly more abundant in the buds and bud-proximal portion of the mother cell plasma membrane. This led us to hypothesize that the distinct plasma membrane localization patterns for these two GTPases might be linked to their distinct functions in promoting polarized growth during different stages of bud growth.

To test this model, we created chimeric forms of the two GTPases to identify the region(s) required for the distinct functions and localization in the cell. Surprisingly, we found that chimeras that exchanged a small region (19 residues of Rho3 and 6 residues of Cdc42) at the extreme N termini of the two proteins resulted in rather dramatic consequence to both the function and localization of these two GTPases. We examined the functional consequences of these chimeras expressed behind either the *CDC42* or *RHO3* promoter present on a low-copy *CEN* plasmid. The ability of each chimera to complement a deletion in the chromosomal copy of *RHO3* or *CDC42* was assessed using a plasmid shuffle assay (see Materials and Methods). The results of the complementation show that the N terminus of Rho3 is critical for its function (Fig. 2B). Rho3, which has had its N terminus replaced with that of Cdc42 (*rho3-NT^{C42}*), no longer complements *rho3*Δ, demon-

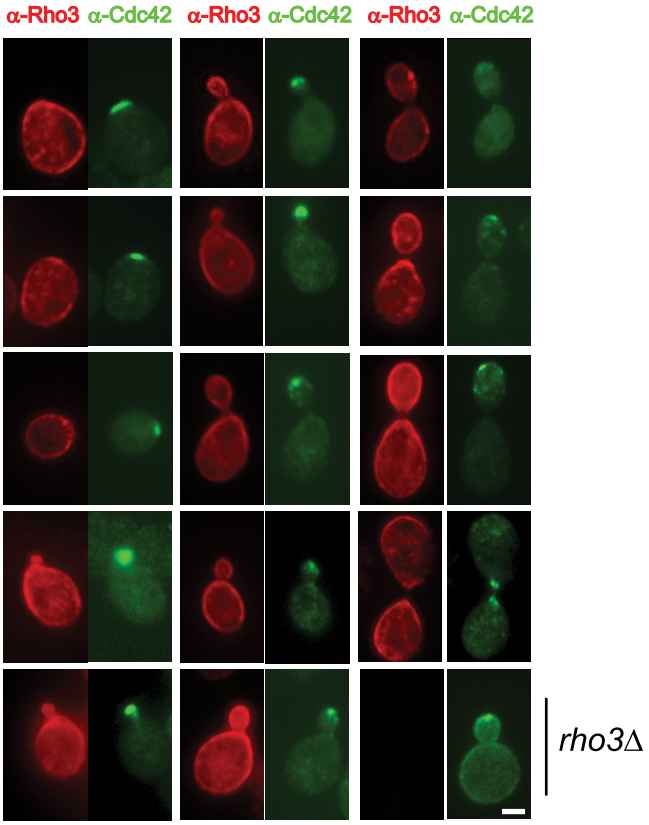

FIG. 1. Localization of Rho3 and Cdc42. Localization of Rho3 and Cdc42 was examined by immunofluorescence microscopy. Each cell was double labeled with mouse anti-Rho3 monoclonal antibody (red pseudocolor) and affinity-purified rabbit anti-Cdc42 polyclonal antibody (green pseudocolor) in a *RHO3* plasmid shuffle strain. Cells containing *rho3D* are used as a negative control for specificity of the Rho3 monoclonal antibody. *rho3*Δ cells were kept alive by the presence of the *CDC42-NT^{R3}* chimera. Cells were grown in selective media, fixed, and processed for immunofluorescence microscopy as described in Materials and Methods. Scale bar, 1 μm.

strating that the N terminus of Rho3 is required for its essential function. Surprisingly, the addition of this region onto Cdc42 converts Cdc42 into a protein, Cdc42-NT^{R3}, that completely complements the loss of Rho3 in the cell. Interestingly, the ability of the Cdc42-NT^{R3} chimera to act as the sole source of Rho3 does not result in a diminution of its ability to act as Cdc42. The Cdc42-NT^{R3} chimera shows no detectable loss of function as the sole source of Cdc42, as it can completely complement *cdc42*Δ. Expression levels of the chimeras were nearly identical to those of their nonchimeric genes (on *CEN* plasmids), suggesting that the switch of function phenotype was not due to the elevated protein levels in the cell. Identical results were obtained for all constructs whether expressed behind the *CDC42* or *RHO3* promoter (data not shown). Since the *CDC42-NT^{R3}* chimeric gene was able to individually complement *rho3*Δ and *cdc42*Δ, we examined whether it could simultaneously act as the sole source of both GTPases by meiotic analysis of a cross between the two *CDC42-NT^{R3}*-complemented knockout strains. The result of this cross clearly demonstrated that while the chimeric gene complemented the individual *rho3* and *cdc42* deletions, it was unable to rescue the segregants predicted to contain both *rho3* and *cdc42* deletions (data not shown).

We then examined the effect of the N-terminal exchange on the localization of the chimeric GTPases by immunofluorescence. Since the Rho3 and Cdc42 antibodies bind to the main body of each GTPase and not to N-terminal domains exchanged in the chimeras, we could monitor the localization of each chimera as the only source of either Rho3 or Cdc42 in the cell. When we examined the staining pattern of Cdc42-NT^{R3} chimera as the sole source of Cdc42 in the cell, we found a striking change in the staining pattern observed with the Cdc42 antibody. The staining pattern, seen in Fig. 2D, is very similar to the dispersed plasma membrane localization of Rho3, and more importantly, not only did this chimeric protein obtain a "Rho3-like" staining pattern; a significant number of cells with small or incipient buds also maintained a "Cdc42-like" staining pattern. Quantitation of the observed staining patterns suggested that roughly 80% of the small-budded cells acquired a localization pattern that resembles both Rho3 and Cdc42. When the Rho3-NT^{C42} chimera was analyzed, we found that the normal Rho3 pattern of plasma membrane staining was lost, and only diffuse cytoplasmic staining was observed. We confirmed the change in plasma membrane localization of the Cdc42-NT^{R3} chimera using a monoclonal antibody against Cdc42. The results, shown in Fig. 2E, demonstrate that the effect of the N terminus of Rho3 on Cdc42 localization is clearly detected by both antibodies. Taken together, these results suggested that the Rho3 N terminus is an important determinate for localization—both in dictating the pattern of localization and in the recruitment of the Rho GTPase to the plasma membrane. We believe that the ability of the Cdc42-NT^{R3} chimera to adopt both "Rho3-like" and Cdc42-like patterns of localization is important for its ability to function as either GTPase in the cell. Therefore, the ability of the N terminus to affect both the function and localization of the associated GTPase gives strong support to the model that localization pattern is critical to the function of these two Rho GTPases in the cell.

The Rho3 N terminus encodes multiple determinants of specificity. To further dissect the mechanism by which the N terminus of Rho3 affected the function and localization of the protein, we carried out an extensive mutagenesis of this domain and examined the effect on localization and function both in the context of the Cdc42-NT^{R3} chimera and in that of wild-type Rho3. The functional studies shown in Fig. 3B demonstrate a requirement for a cysteine at position 5 and two adjacent residues at positions 3 and 4 in the ability of this domain to affect a switch of function phenotype in the context of the Cdc42-NT^{R3} chimera. The cysteine residue at position five has previously been shown to be palmitoylated (24). Consistent with this notion, we find that the Rho3-C5A protein no longer demonstrates plasma membrane staining, and the protein is largely absent from the membrane pellet fraction following cell fractionation (Fig. 3D and E). The effect of the alanine mutations at position 3,4 (A3,4) (from phenylalanine and leucine) appears to have a similar effect on localization and fractionation (Fig. 3D and E) and therefore may be a component of the recognition sequence used by the palmitoyltransferase.

We next examined the effect of the palmitoylation site mu-

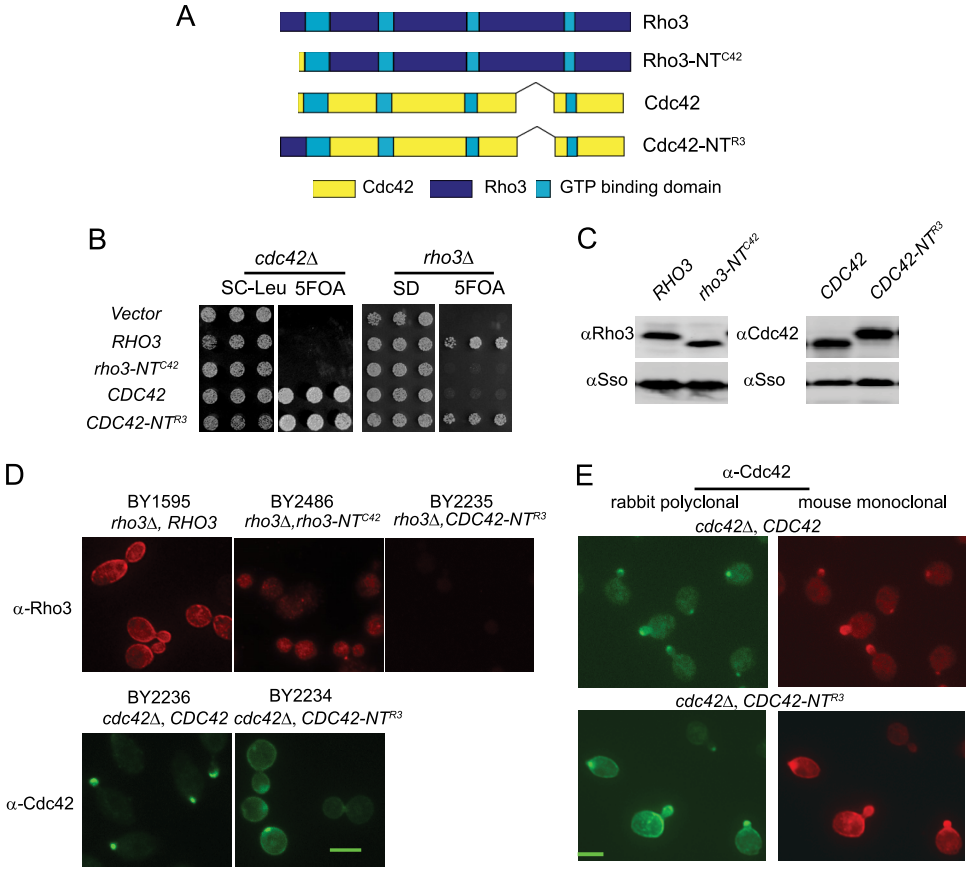

FIG. 2. The N terminus of Rho3 is necessary and sufficient for its function and localization. (A) Schematic representations of *RHO3*, *RHO3* with the N terminus of *CDC42* (*rho3-NT*^{C42}), *CDC42*, and *CDC42* with the N terminus of *RHO3* (*CDC42-NT*^{R3}). (B) *RHO3*, *rho3-NT*^{C42}, *CDC42*, and *CDC42-NT*^{R3} were transformed into a *RHO3* plasmid shuffle strain or a *CDC42* plasmid shuffle strain on a *CEN HIS3* plasmid. The growth of three independent colonies was shown under restrictive conditions where the wild-type *RHO3-URA3* or the *CDC42-URA3* plasmid was lost by counterselection on 5-FOA plates. (C) Whole-cell lysates were prepared of strains with *CDC42* or *CDC42-NT*^{R3} as the only source for *CDC42* and strains with *RHO3* or *rho3-NT*^{C42} as the only source for *RHO3*. Lysates were subjected to SDS-PAGE analysis and blotted with Cdc42 or Rho3 monoclonal antibodies. Since *rho3-NT*^{C42} cannot function as the only copy of *RHO3* in the cell, the gain-of-function chimera *CDC42-NT*^{R3} was introduced into the cell to maintain viability. (D) Cells containing plasmids encoding *RHO3*, *rho3-NT*^{C42}, *CDC42*, and *CDC42-NT*^{R3} as the only source of Rho3 or Cdc42 in the cell were grown at 25°C, fixed, and processed for immunofluorescence. Mouse monoclonal antibody against Rho3 and rabbit polyclonal antibody against Cdc42 were used as described in Materials and Methods. The yeast strains (BY2235, BY2486 [see Table 1]) contain *rho3*Δ complemented by *CDC42-NT*^{R3} in addition to the chimera shown to allow us to examine the localization of noncomplementing forms of Rho3. The anti-Rho3 MAb does not recognize the Cdc42-NT^{R3} protein. (E) Cells containing *CDC42* or *CDC42-NT*^{R3} as the only source of *CDC42* were grown at 25°C and processed for double-label immunofluorescence with affinity-purified rabbit polyclonal antibody and a mouse monoclonal antibody, both against Cdc42. Scale bar, 2 μm.

tations on the ability of the N terminus of Rho3 to affect the localization pattern of the Cdc42-NT^{R3} chimera. Interestingly, we found that the cysteine-to-alanine mutation in this chimera resulted in a nearly complete loss of the Rho3-like staining pattern and instead revealed a staining pattern almost identical to that seen for wild-type Cdc42. Thus, palmitoylation at the N terminus of Rho3 appears to be a critical signal in redirecting the pattern of localization from a highly polarized "Cdc42-like" pattern to the more dispersed pattern seen for Rho3.

Unexpectedly, while loss of palmitoylation was required for the switch-of-function phenotype, it was dispensable for function in the context of wild-type Rho3. Although these mutations resulted in a significantly more soluble protein (as judged by fluorescence and fractionation), presumably enough Rho3 is associated with the membrane to provide the minimal requirements for Rho3 function.

Analysis of DHHC family palmitoyltransferases on Rho3 membrane localization. Protein palmitoylation is thought to be carried out primarily by members of the DHHC family of proteins (16, 18). Yeast contains seven members of the DHHC family, one of which, Erf2, had previously been implicated in palmitoylation of the Rho3 N terminus (24). While *erf2*Δ was the only DHHC family member that resulted in a clear loss of Rho3 palmitoylation, it was proposed that other DHHC family members were likely to be involved as well, since loss of *erf2* results in only a partial reduction in the palmitoylation of Rho3 (24).

Since palmitoylation of the N terminus is essential for the Cdc42-NT^{R3} chimera to function as the sole source of Rho3, this allowed us to ask whether a specific member(s) of the DHHC family of palmitoyltransferases was required for the Cdc42-NT^{R3} switch-of-function phenotype. To examine

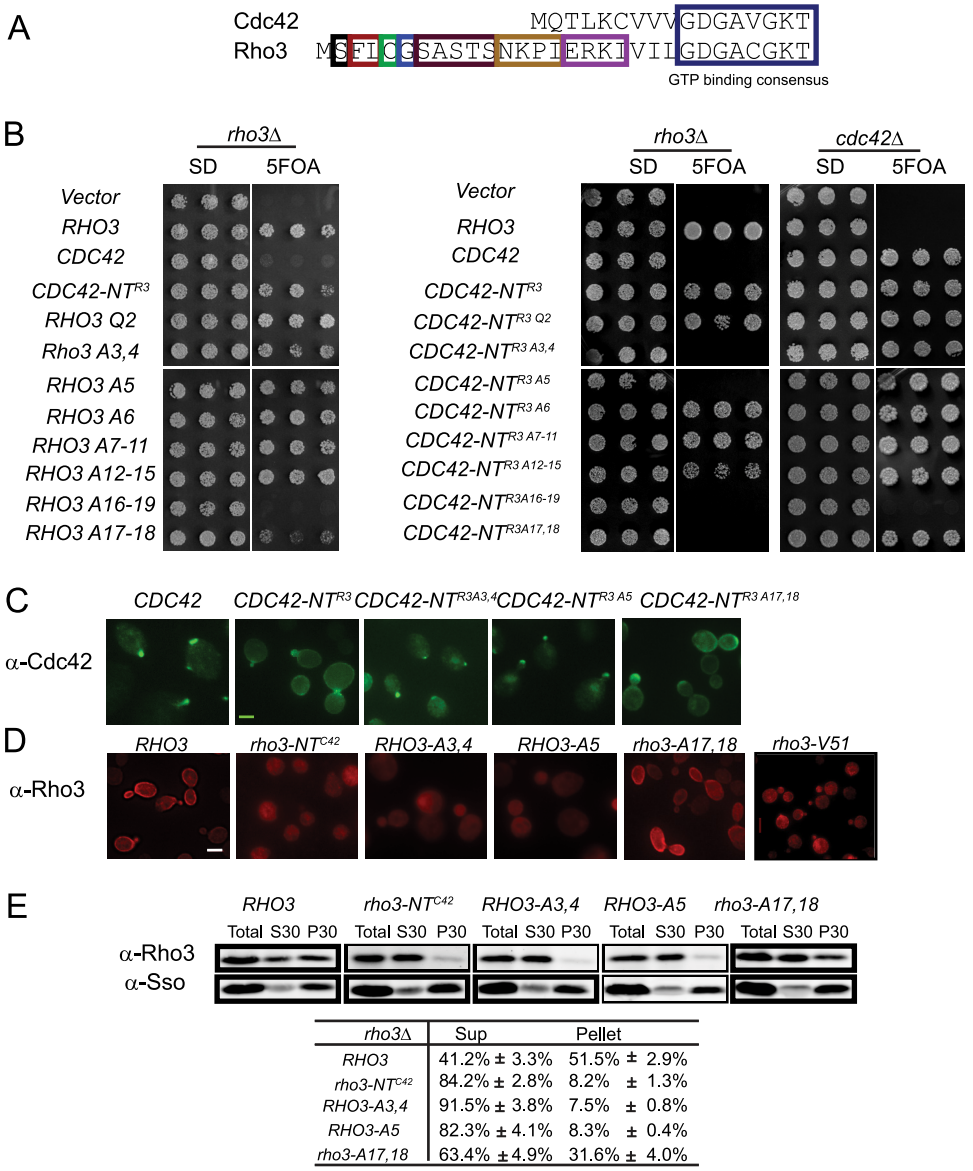

rho3Δ	Sup	Pellet
RHO3	41.2% ± 3.3%	51.5% ± 2.9%
rho3-NTC42	84.2% ± 2.8%	8.2% ± 1.3%
RHO3-A3,4	91.5% ± 3.8%	7.5% ± 0.8%
RHO3-A5	82.3% ± 4.1%	8.3% ± 0.4%
rho3-A17,18	63.4% ± 4.9%	31.6% ± 4.0%

FIG. 3. The N terminus of *RHO3* contains two elements that are important for its function and localization. (A) Single residues or a group of residues were mutated to alanine at the N terminus of Rho3. Mutations are depicted with colored boxes. (B) *CDC42* and both *RHO3* and the *CDC42-NT^{R3}* chimera with the corresponding N-terminal mutants were transformed into a *RHO3* plasmid shuffle strain on a *CEN HIS3* plasmid. The ability of the mutants to complement *rho3*Δ was analyzed on 5-FOA plates where the wild-type *RHO3-URA3* plasmid is lost. (C) *CDC42*, *CDC42-NT^{R3}*, *CDC42-NT^{R3}A3,4*, *CDC42-NT^{R3}A5*, and *CDC42-NT^{R3}A17,18* were first transformed into a *CDC42* plasmid shuffle strain and then grown on 5-FOA plates to evict the original *CDC42* plasmid. Immunofluorescence was performed using anti-Cdc42 polyclonal antibody as described in Materials and Methods. (D) Yeast cells containing *RHO3*, *rho3-NT^{C42}*, *RHO3-A3,4*, *RHO3-A5*, and *rho3-A17,18* on *CEN-HIS3* plasmids or an integrated copy of *rho3-V51* (2) were grown to mid-log phase at 25°C, fixed, and processed for immunofluorescence using anti-Rho3 MAb5-41. Note the *rho3-V51* mutant cells were grown in rich medium and hence are smaller. Scale bar: 2 μm. (E) Yeast cells containing *RHO3*, *rho3-NT^{C42}*, *RHO3-A3,4*, *RHO3-A5*, and *rho3-A17,18* as the only source of *RHO3* were grown at 25°C, spheroplasted, lysed, and spun at 30,000 × *g* to separate the cytosolic and the membrane fraction. Samples of total cell lysates (total), supernatant (Sup, S30), and pellet (P30) were subjected to SDS-PAGE analysis and Western blot analysis. *rho3-NT^{C42}* (BY2486) and *rho3-A17,18* (BY2487) strains contain a *CDC42-NT^{R3}* on a *CEN-HIS3* plasmid to maintain the viability of the cell.

this point further, we constructed strains containing deletions of each of the seven DHHC family members in the context of the *RHO3* plasmid shuffle strain. We then examined the effect of loss of each palmitoyltransferase on the ability of the *CDC42-NT^{R3}* chimera to complement the *rho3*Δ, following growth on 5-FOA medium. Surprisingly, we found that *erf2*Δ, encoding a palmitoyltransferase previously reported to be a significant source of palmitoyltransferase activity on Rho3 (24), had only a modest effect on the ability of the chimera to complement *rho3*Δ. Loss of another palmitoyltransferase, Pfa4, also showed a similar partial effect on complementation. In contrast to the modest effect on complementation in the presence of *erf2*Δ and *pfa4*Δ, loss of the Akr1 transferase was found to be essential for the switch of function, as loss of this DHHC family member completely

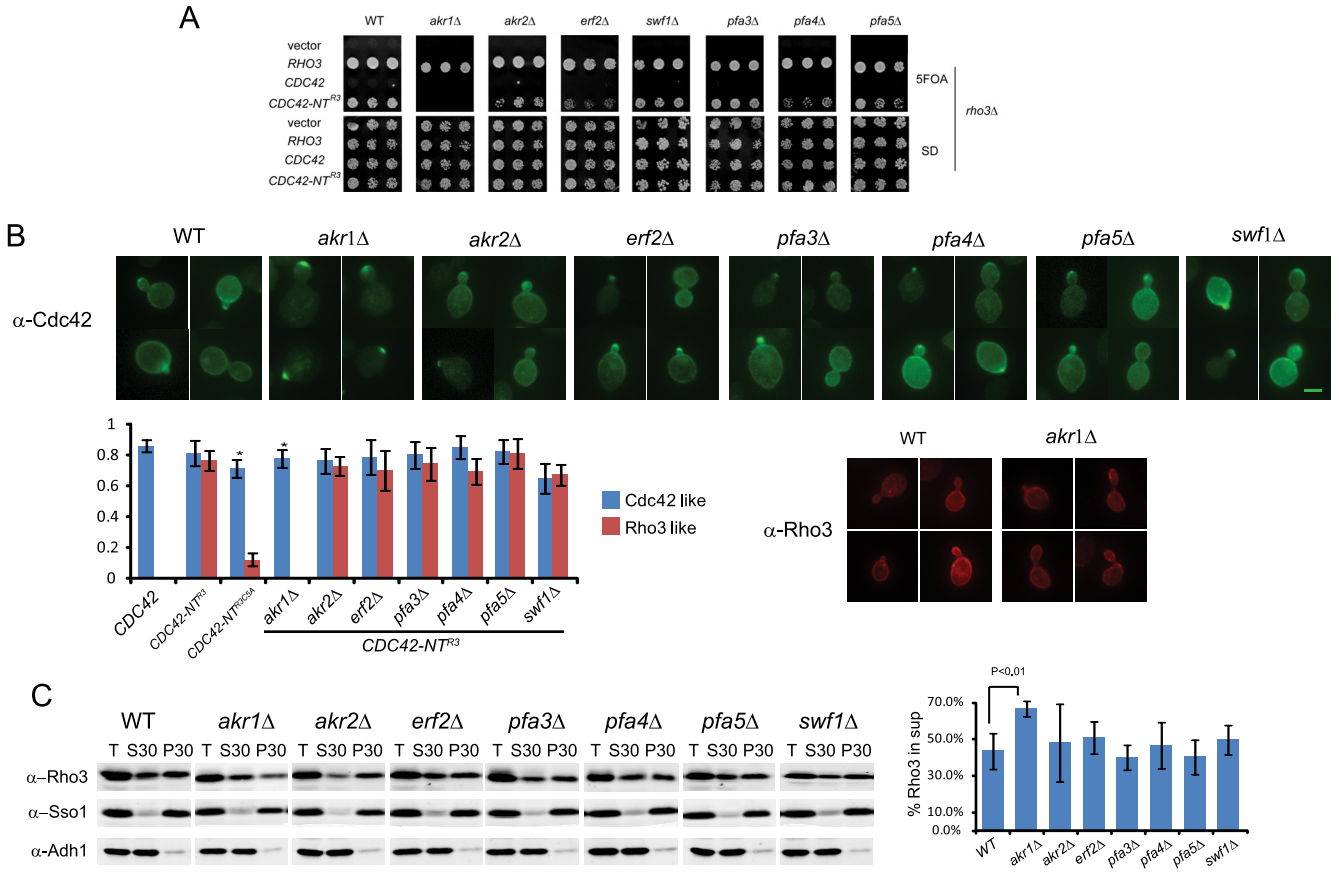

FIG. 4. Akr1 is required for the membrane association of Rho3 and the switch of function and localization phenotype of *Cdc42-NT^{R3}*. (A) *RHO3*, *CDC42*, and *CDC42-NT^{R3}* were transformed into *RHO3* plasmid shuffle strains in which each palmitoyltransferase was deleted. The growth of three independent colonies was shown under restrictive conditions where the wild-type *RHO3-URA3* plasmid was lost by counterselection on 5-FOA plates. (B) Wild-type (WT) cells or cells deleted for each palmitoyltransferase, bearing *CDC42-NT^{R3}* as the only source for *CDC42*, were fixed and processed for immunofluorescence using anti-Cdc42 polyclonal antibody as described in Materials and Methods. Approximately 200 cells were randomly selected and scored for Cdc42-like bud tip localization in small-budded cells or Rho3-like dispersed plasma membrane localization in small- and large-budded cells. The bar graphs represent the percentage of cells with either "Cdc42-like" localization or the "Rho3-like" localization pattern. Quantitations were performed for four sets of immunofluorescence images, with error bars representing the standard deviations. Wild-type or *akr1*Δ cells were grown at 25°C and processed for immunofluorescence with mouse monoclonal antibody against Rho3. (C) Wild-type cells or cells deleted for each palmitoyltransferase were grown at 25°C, spheroplasted, lysed, and spun at 30,000 × *g* to separate the cytosolic and the membrane fraction. Equal volumes of total cell lysates (total) and supernatant (S30) and pellet (P30) fractions were subjected to SDS-PAGE analysis and blotted with anti-Rho3 monoclonal antibody. As controls, the anti-Sso1/2 antibody and the anti-Adh1 antibody (Abcam Inc.) were used to detect the plasma membrane fraction (P30) and the cytosolic fraction (S30). The bar graph represents the quantitation of results of three independent experiments. Data were analyzed by a two-tailed Student *t* test, with error bars representing standard deviations.

blocked the ability of *CDC42-NT^{R3}* to complement growth. Deletion of the other four DHHC family members showed no detectable effect on complementation of *rho3*Δ by *CDC42-NT^{R3}*.

To determine if the effect caused by the loss of *akr1* was due to a change in the localization of the chimeric protein, we examined the staining pattern of the Cdc42-NT^{R3} chimera as the only source of Cdc42 in an *akr1*Δ background. The results demonstrate that as in the C5A mutant form of this chimera, the Cdc42-NT^{R3} GTPase, an *akr1*Δ background is found only in the highly polarized staining pattern typical of Cdc42 and is unable to adopt the "Rho3-like" staining pattern seen for this chimera in wild-type cells (Fig. 4B). The staining pattern of this chimera in the other six DHHC knockout strains showed no significant difference from that seen in wild-type cells.

To further delineate the role of these palmitoyltransferases in determining the localization of Rho3 in the cell, we examined the effects of deleting each of the DHHC proteins on the association of Rho3 with membranes following subcellular fractionation. The results, shown in Fig. 4C, demonstrate that six of the seven DHHC deletion mutants—including *erf2*Δ—showed no significant loss of membrane association. However, consistent with the genetic requirement for *AKR1* described above, the *akr1*Δ strain shows a significant ($P < 0.01$) increase in the fraction of Rho3 that was soluble after 30,000 × *g* centrifugation (Fig. 4C). It is important to note that although the solubility of Rho3 has increased in the *akr1*Δ strain, there is still more protein associated with the pellet than a in C5A mutant (40% versus 8.3%), consistent with the notion that multiple palmitoyltransferases are likely to be involved in palmitoylating Rho3. Taken together, these data strongly sug-

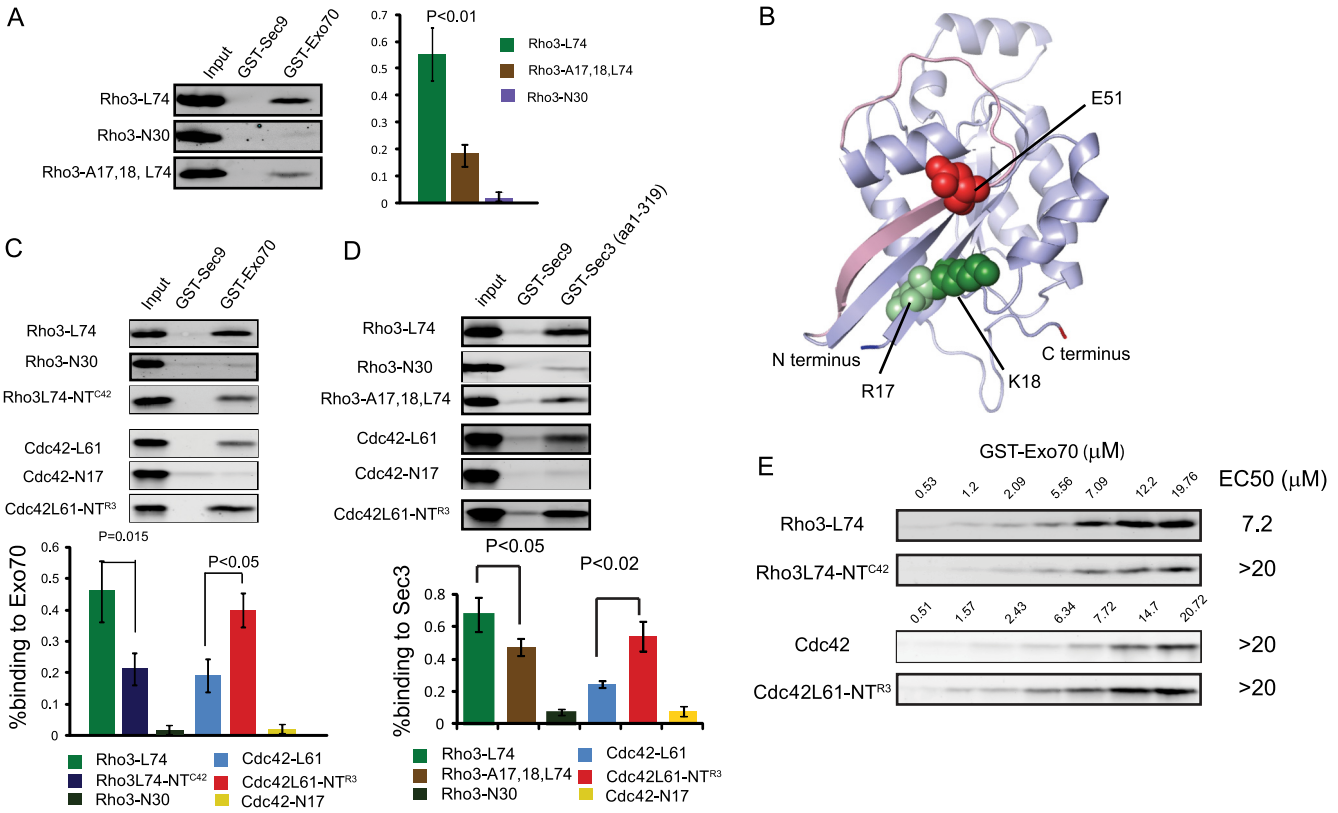

FIG. 5. The N terminus of Rho3 and Cdc42 determines the affinity of their interaction with Exo70. (A) GST-Sec9 (aa 402 to 651; control) and GST-Exo70 (full length) were purified from bacteria and immobilized on glutathione-Sepharose beads. Yeast lysates overexpressing GTP-bound Rho3 (Rho3-L74) or GTP-bound Rho3-A17,18 (Rho3-A17,18, L74) were expressed behind a galactose-inducible promoter. The binding experiments were performed as described in the text. The bar graph on the right panel represents the quantitation of the Western blot. Data were analyzed by a two-tailed Student *t* test, with error bars representing standard deviations of results from four independent experiments. (B) Homology model for yeast Cdc42 in a slate blue cartoon representation. The model is based on the template of human Cdc42 (1GRN). The N terminus, C terminus, and switch I region of Cdc42 are colored dark blue, red, and light pink, respectively. Residues 4 and 5 (leucine and lysine) in Cdc42, which correspond to residues 17 and 18 (arginine and lysine) in Rho3, are represented as spheres in light green. Residue 38 (aspartic acid) of Cdc42, which corresponds to residue 51 (glutamic acid) in Rho3, is represented as spheres in light pink. (C) Yeast lysates overexpressing GTP-locked forms of Rho3, Cdc42, the gain-of-function chimera Cdc42-NT^{R3}, and the loss-of-function chimera Rho3-NT^{C42} were expressed behind a galactose-inducible promoter in yeast. Lysates obtained from these strains were used in the binding experiments. The input represents 1% binding. The bar graph below the gel represents the quantitation of the Western blots using the Odyssey infrared imaging system. Data were analyzed by the two-tailed Student's *t* test, with error bars representing standard deviations of results from five independent experiments. (D) Lysates containing the indicated Rho GTPase were incubated with either control GST-Sec9 (aa 402 to 651) or GST-Sec3 (aa 1 to 319)-containing beads and analyzed as for panel A. (E) Yeast lysate was incubated with increasing concentrations of GST-Exo70 as indicated above the blot. Samples were subjected to Western blot analysis using monoclonal antibodies against Rho3 and Cdc42. The predicted EC_{50} is indicated at the right.

gest the involvement of a novel palmitoyltransferase, Akr1, in palmitoylation of the N terminus of Rho3 and further demonstrate the importance of N-terminal palmitoylation of Rho3 in determining the distinct function and localization of Rho3 in the cell.

The N-terminal region of Rho3 and Cdc42 determines the strength of binding to Exo70. A second important element in the Rho3 N terminus was identified by mutation of a pair of basic residues at positions 17 and 18, arginine and lysine. When these residues were replaced with alanine in the context of either Rho3 or the Cdc42-NT^{R3} chimera, the ability of either protein to rescue the loss of *rho3*Δ in the cell was completely lost. When we examined the effect of these mutations on the localization of Rho3 or Cdc42-NT^{R3}, we found that the mutant proteins localized similarly to the wild-type form of the proteins (Fig. 3C and D), although there was a slight reduction in the amount of Rho3 protein associated with the membrane pellets by fractionation (Fig. 3E). The strong loss-of-function phenotypes associated with mutations at these residues suggested that they might play a role in the interaction of Rho3 with an upstream or downstream component of its signaling pathway. Exo70 is a critical downstream effector for both Rho3 and Cdc42 signaling to the exocytic apparatus, and both prenylated Rho3 and Cdc42 bind to Exo70 in a manner that is both GTP and effector domain dependent (29). We made use of this assay to examine the effects of the A17,18 mutations on the ability of GTP-locked Rho3 (Rho3-L74) to bind to the effector protein Exo70. The results, shown in Fig. 5A, demonstrate that Exo70 binding to GTP-bound Rho3 is almost completely lost in the presence of the A17,18 mutations. By modeling the structure of Rho3 based on the existing structure of Cdc42 (20), it is apparent that Rho3 residues 17 and 18 are

likely to be in close proximity (10 to 12 Å) to the effector domain in the active GTP-bound form of the protein (Fig. 5B). Therefore, these residues in the N terminus of Rho3 likely represent part of the binding surface used by Exo70 in its interaction with the GTP-bound forms of Rho3.

To further examine whether the localization of Rho3 depends on its ability to bind to its effectors, we made use of a previously characterized effector domain mutant, *rho3-V51*, which is defective in promoting exocytosis and has a significantly reduced affinity for Exo70 (2, 29). Immunofluorescence using monoclonal Rho3 antibody in this mutant revealed a dispersed plasma membrane staining pattern similar to that for wild-type Rho3. Combined with the similar result from the *rho3-A17,18* mutant, this suggests that the "Rho3-like" plasma membrane localization pattern for Rho3 is likely to be independent of effector binding.

These results suggested that in addition to the function of the N terminus of Rho3 in determining its unique localization pattern, this region likely has a role in providing elements involved in binding to the downstream effector Exo70. We therefore examined the effect of exchanging the N termini of Rho3 and Cdc42 on the binding to Exo70. The results, shown in Fig. 5C, demonstrate that the Rho3 N terminus promotes the interaction with Exo70 relative to that of the homologous region of Cdc42. In particular, the binding to GTP-locked Rho3-NT^{C42} is significantly reduced relative to that of Rho3, and the binding to GTP-locked Cdc42 is significantly improved by the presence of the Rho3 N terminus. To examine the effect of these regions on the relative affinity of each GTPase for Exo70, we performed equilibrium binding assays over a large range of concentrations of recombinant Exo70. The extent of interaction with GTP-locked forms of Rho3, Cdc42, and each of the N-terminal chimeras was monitored by quantitative Western blot analysis as shown in Fig. 5E. The binding results were used to estimate the 50% effective concentration (EC_{50})—a measure of the apparent affinity observed between each GTPase and Exo70 in this assay. These binding isotherms demonstrate that the Rho3 has a significantly higher affinity for Exo70, with its native N terminus, than for the N-terminal domain of Cdc42 (7 μM versus over 20 μM) and that while the EC_{50} for both Cdc42 and Cdc42-NT^{R3} was too low to be accurately estimated by this procedure, it was clear that at the binding of Cdc42-NT^{R3} it was consistently higher than that of Cdc42 in this assay. This demonstrates that the N terminus of Rho3 plays an important role in determining the strength of interaction between the Rho GTPase and its effector Exo70. This may play an important role in allowing Rho3 to signal to the exocyst complex during the more dispersed (i.e., less concentrated) polarized growth conditions present during isotropic growth of larger-budded cells, where both the GTPase and its effector are likely to be present in significantly more dilute concentrations on the plasma membrane.

We also examined the ability of Rho3 and Cdc42 to interact with another potential Rho effector within the exocyst complex, Sec3, utilizing an assay identical to that described above for Exo70. The N terminus of Sec3 (aa 1 to 319) has been shown previously to bind to Rho1 and Cdc42 (8, 32), but interaction with Rho3 has not been examined. We therefore examined the ability of different forms of Rho3 and Cdc42 to interact with GST-Sec3-NT (aa 1 to 319). The results, shown in Fig. 5D, demonstrate the expected nucleotide-dependent interaction with GTP-locked Cdc42 (Cdc42-L61) but not GDP-Cdc42 (Cdc42-N17) and unexpectedly also demonstrate GTP-dependent binding to activated Rho3 (Rho3-L74) but not GDP-Rho3 (Rho3-N30). Interestingly, as with the interaction with Exo70, we find that this interaction is significantly reduced by the presence of the A17,18 mutations in activated Rho3 and the interaction with activated Cdc42 is significantly enhanced by the addition of the N terminus of Rho3. This suggests that the switch of function phenotype of the Cdc42-NT^{R3} chimera may involve recognition by multiple subunits of the exocyst by increasing its avidity for interaction with both the Exo70 and Sec3 components of the complex.

DISCUSSION

The pattern of plasma membrane localization for Rho/Cdc42 GTPase family members is thought to play a critical role in determining and maintaining cell polarity. Here, using yeast as a model, we provide direct evidence that the plasma membrane localization pattern of two Rho GTPases is critical for each of their functions in promoting bud growth at distinct times during the cell cycle. Using chimeric forms of Rho3 and Cdc42, we demonstrate that the N-terminal domain of these two GTPases defines both of these functions. We find that the Rho3 pattern of localization is critical for its function in promoting polarized exocytosis—especially in larger-budded cells where Cdc42 polarity is lost. In particular, palmitoylation of Rho3 at C5 in the N-terminal domain is required for adopting its dispersed plasma membrane staining and for allowing a pool of Cdc42 to enter into a "Rho3-like" localization pattern. The precise mechanism by which palmitoylation of Rho3 is linked to this pattern of plasma membrane localization is presently unknown. We find evidence that DHHC family palmitoyltransferases play a role in these events. Previous studies implicated the Erf2 palmitoyltransferase in modification of Rho3; however, significant levels of palmitoylation were still detectable in *erf2*Δ strains (24). We have found that deletion of the gene encoding this enzyme has only a minor effect on the switch-of-function property associated with the Cdc42-NT^{R3} chimera. Therefore, other palmitoyltransferases likely play a role in determining the dispersed plasma membrane localization pattern seen for Rho3. One of the unexpected results of this work was the finding that the Akr1 enzyme plays an essential role in the localization of Rho3. The results of this work are consistent with the notion that Akr1 directly palmitoylates the N terminus of Rho3, since it is required for the ability of the Cdc42-NT^{R3} chimera to function as Rho3, for the chimera to switch localization to the "Rho3-like" pattern, and for the normal levels of membrane association of Rho3 following subcellular fraction.

A previous study (22) suggested that a small pool of Rho3 may sometimes be found in a bud tip localization pattern and that this pattern could be enhanced by utilizing a cold-sensitive allele of Rho3 with elongated buds. However, it is important to note that this pattern was observed under conditions that were significantly different from those we have employed in this study. In particular, this previous study utilized both a strong inducible promoter (*GAL7*), which would be expected to result in Rho3 that is highly overexpressed, and mutant forms of

Rho3 (Rho3-E129 and Rho3-E129, A131) predicted to alter the nucleotide cycle of the protein. It is possible that either overexpression or mutational change in Rho3 (or the combination) results in the partial bud tip localization observed in this study. In the present study, all constructs examined were expressed on single-copy (CEN) plasmids behind the native *RHO3* (or *CDC42*) promoter and did not contain mutations predicted to affect the GTPase cycle. We also observed the dispersed "Rho3-like" plasma membrane staining pattern with multiple antibody probes. Wild-type Rho3 was detected with the anti-Rho3 monoclonal antibody, while a strikingly similar pattern was detected for the Cdc42-NT^{R3} chimera with both polyclonal anti-Cdc42 antibody and a mouse monoclonal antibody for Cdc42 (Fig. 2E). Taken together, these results suggest that the dispersed plasma membrane staining pattern represents the authentic localization for Rho3 in the cell when expressed at normal levels.

In contrast to the consistently dispersed pattern of localization found for Rho3, Cdc42 is tightly polarized to bud tips during bud emergence; however, Cdc42 polarization is lost as the bud enlarges. This pattern of localization appears to require a set of signals distinct from that of Rho3; these signals are likely to reside in the C-terminal portion of the protein. In addition to the C-terminal prenylation (CAAX) signal, a stretch of five basic residues, known as a polybasic region, is present at the C terminus of Cdc42. The pattern of localization observed for Cdc42 closely mirrors the pattern observed for many proteins which ride to the plasma membrane along with polarized delivery of post-Golgi secretory vesicles. This list includes Sec4, Sec2, Myo2, and most of the subunits of the exocyst complex (4, 7). Consistent with this notion, Cdc42 has itself been suggested to be associated with post-Golgi secretory vesicles during cell fractionation (27), and its polarized localization is rapidly lost with a block in polarized secretion (15, 32). The switch of function chimera, Cdc42-NT^{R3}, appears to have the ability to adopt both "Rho3-like" and "Cdc42-like" patterns of localization. This suggests that the pathways that mediate these two localization patterns operate independently of each other. The effects of the palmitoylation site mutation on the localization of Cdc42-NT^{R3} support this view, as we see that the loss of Rho3 localization has no effect on the ability of this protein to demonstrate normal Cdc42 localization.

Although Cdc42 is likely to arrive at the plasma membrane of actively growing cells through association with secretory vesicles, the mechanism by which Rho3 is delivered to the plasma membrane is not known. In this light it is interesting to note that the Akr1 enzyme has been localized to the Golgi apparatus (23) and Erf2 has been reported to be present primarily in the endoplasmic reticulum (3). This suggests that palmitoylated Rho3 is likely to traffic from an intracellular membrane before adopting its final dispersed pattern of localization on the plasma membrane. Preliminary work from our laboratory suggests that, unlike Cdc42 localization, Rho3 localization is unaffected by a block in Golgi apparatus-to-surface trafficking and therefore likely utilizes a pathway which is independent of the classical secretory pathway. This may involve a mechanism(s) related to yeast Ras2, which also is thought to be palmitoylated at intracellular membranes yet adopts a dispersed plasma membrane localization independent of the secretory pathway (16).

In addition to giving insight into two distinct mechanisms for localization of Rho/Cdc42 GTPases, this work demonstrates the importance of effector binding to the specific function of these two GTPases in the cell. This is particularly evident for Rho3, which appears to have evolved a relatively high-affinity means for interacting with the Exo70 component of the exocyst. Rho3 plays a critical role in promoting secretion in larger-budded cells, where the exocyst effector complex is significantly less concentrated than its highly polarized pattern in emerging buds. Consequently, the local concentrations in which Rho3 must engage its target are likely to be considerably more dilute at this point in bud growth than during the highly polarized exocytic delivery that occurs during bud emergence. In contrast, Cdc42 appears to have evolved a lower-affinity means of interacting with Exo70, which might have evolved to match the very high local concentrations of both Cdc42 and the exocyst during bud emergence. This lower-affinity interaction between Cdc42 and Exo70 does not appear to be required, as we find no evidence of polarity or cell shape problems in cells when the higher-affinity Cdc42-NT^{R3} construct is present as the sole source of Cdc42 (unpublished observation). For Rho3, however, the parallel result is not the case, as we find that the Cdc42-NT^{R3}A17,18 mutant is able to be properly localized as Rho3 but cannot function as Rho3 due to a reduced affinity of the GTPase for Exo70. Therefore, localization of an otherwise fully functional Rho GTPase, by itself, is not sufficient to provide Rho3 function.

It is clear that the N terminus of Rho3 plays a very important role in regulating its specific function in the cell. Remarkably, it does this by both specifying a dispersed pattern of localization on the plasma membrane and increasing the avidity of binding to the downstream effector. Both properties of the N terminus appear to play an important role in how Rho3 regulates vesicle docking and fusion during isotropic growth of large-budded cells. This is in contrast to how Cdc42 acts during bud emergence, when a concentrated patch of Cdc42 and exocyst complex helps to promote a high flux of exocytosis at highly polarized bud tips. As the bud enlarges, both Cdc42 and exocyst polarization are lost and Rho3 is left as the primary regulator of exocyst-dependent docking and fusion events.

ACKNOWLEDGMENTS

We are grateful to Brenda Temple (University of North Carolina Structural Bioinformatics Core) for assistance with structure modeling of Rho3 and Courtney Turner for technical assistance. We thank Bradley Bone (UNC Immunology Core) and Daniel Lew (Duke University) for help in the isolation and characterization of the Rho3 and Cdc42 monoclonal antibodies. We thank Guendalina Rossi for helpful discussions and critical reading of the manuscript.

This work was supported by grants from the Mathers Charitable Foundation and the National Institutes of Health (GM54712) to P. J. Brennwald.

REFERENCES

1. **Adamo, J. E., J. J. Moskow, A. S. Gladfelter, D. Viterbo, D. J. Lew, and P. J. Brennwald.** 2001. Yeast Cdc42 functions at a late step in exocytosis, specifically during polarized growth of the emerging bud. J. Cell Biol. **155:**581–592.
2. **Adamo, J. E., G. Rossi, and P. Brennwald.** 1999. The Rho GTPase Rho3 has a direct role in exocytosis that is distinct from its role in actin polarity. Mol. Biol. Cell **10:**4121–4133.
3. **Bartels, D. J., D. A. Mitchell, X. Dong, and R. J. Deschenes.** 1999. Erf2, a novel gene product that affects the localization and palmitoylation of Ras2 in *Saccharomyces cerevisiae*. Mol. Cell. Biol. **19:**6775–6787.
4. **Boyd, C., T. Hughes, M. Pypaert, and P. Novick.** 2004. Vesicles carry most

exocyst subunits to exocytic sites marked by the remaining two subunits, Sec3p and Exo70p. J. Cell Biol. **167:**889–901.
5. **Brennwald, P., and P. Novick.** 1993. Interactions of three domains distinguishing the Ras-related GTP-binding proteins Ypt1 and Sec4. Nature **362:** 560–563.
6. **Ghomashchi, F., X. Zhang, L. Liu, and M. H. Gelb.** 1995. Binding of prenylated and polybasic peptides to membranes: affinities and intervesicle exchange. Biochemistry **34:**11910–11918.
7. **Goud, B., A. Salminen, N. C. Walworth, and P. J. Novick.** 1988. A GTP-binding protein required for secretion rapidly associates with secretory vesicles and the plasma membrane in yeast. Cell **53:**753–768.
8. **Guo, W., F. Tamanoi, and P. Novick.** 2001. Spatial regulation of the exocyst complex by Rho1 GTPase. Nat. Cell Biol. **3:**353–360.
9. **Guthrie, C., and G. Fink (ed.).** 1991. Guide to yeast genetics and molecular biology. Academic Press, San Diego, CA.
10. **Hancock, J. F., H. Paterson, and C. J. Marshall.** 1990. A polybasic domain or palmitoylation is required in addition to the CAAX motif to localize p21ras to the plasma membrane. Cell **63:**133–139.
11. **He, B., F. Xi, J. Zhang, D. TerBush, X. Zhang, and W. Guo.** 2007. Exo70p mediates the secretion of specific exocytic vesicles at early stages of the cell cycle for polarized cell growth. J. Cell Biol. **176:**771–777.
12. **Heo, W. D., T. Inoue, W. S. Park, M. L. Kim, B. O. Park, T. J. Wandless, and T. Meyer.** 2006. PI(3,4,5)P3 and PI(4,5)P2 lipids target proteins with polybasic clusters to the plasma membrane. Science **314:**1458–1461.
13. **Horton, R. M., H. D. Hunt, S. N. Ho, J. K. Pullen, and L. R. Pease.** 1989. Engineering hybrid genes without the use of restriction enzymes: gene splicing by overlap extension. Gene **77:**61–68.
14. **Hougland, J. L., C. L. Lamphear, S. A. Scott, R. A. Gibbs, and C. A. Fierke.** 2009. Context-dependent substrate recognition by protein farnesyltransferase. Biochemistry **48:**1691–1701.
15. **Irazoqui, J. E., A. S. Gladfelter, and D. J. Lew.** 2003. Scaffold-mediated symmetry breaking by Cdc42p. Nat. Cell Biol. **5:**1062–1070.
16. **Linder, M. E., and R. J. Deschenes.** 2007. Palmitoylation: policing protein stability and traffic. Nat. Rev. Mol. Cell Biol. **8:**74–84.
17. **Maurer-Stroh, S., and F. Eisenhaber.** 2005. Refinement and prediction of protein prenylation motifs. Genome Biol. **6:**R55.
18. **Mitchell, D. A., A. Vasudevan, M. E. Linder, and R. J. Deschenes.** 2006. Protein palmitoylation by a family of DHHC protein S-acyltransferases. J. Lipid Res. **47:**1118–1127.
19. **Moores, S. L., M. D. Schaber, S. D. Mosser, E. Rands, M. B. O'Hara, V. M. Garsky, M. S. Marshall, D. L. Pompliano, and J. B. Gibbs.** 1991. Sequence dependence of protein isoprenylation. J. Biol. Chem. **266:**14603–14610.
20. **Nassar, N., G. R. Hoffman, D. Manor, J. C. Clardy, and R. A. Cerione.** 1998. Structures of Cdc42 bound to the active and catalytically compromised forms of Cdc42GAP. Nat. Struct. Biol. **5:**1047–1052.
21. **Nelson, W. J.** 2009. Remodeling epithelial cell organization: transitions between front-rear and apical-basal polarity. Cold Spring Harb. Perspect. Biol. **1:**a000513.
22. **Robinson, N. G., L. Guo, J. Imai, E. A. Toh, Y. Matsui, and F. Tamanoi.** 1999. Rho3 of *Saccharomyces cerevisiae*, which regulates the actin cytoskeleton and exocytosis, is a GTPase which interacts with Myo2 and Exo70. Mol. Cell. Biol. **19:**3580–3587.
23. **Roth, A. F., Y. Feng, L. Chen, and N. G. Davis.** 2002. The yeast DHHC cysteine-rich domain protein Akr1p is a palmitoyl transferase. J. Cell Biol. **159:**23–28.
24. **Roth, A. F., J. Wan, A. O. Bailey, B. Sun, J. A. Kuchar, W. N. Green, B. S. Phinney, J. R. Yates III, and N. G. Davis.** 2006. Global analysis of protein palmitoylation in yeast. Cell **125:**1003–1013.
25. **Roumanie, O., H. Wu, J. N. Molk, G. Rossi, K. Bloom, and P. Brennwald.** 2005. Rho GTPase regulation of exocytosis in yeast is independent of GTP hydrolysis and polarization of the exocyst complex. J. Cell Biol. **170:**583–594.
26. **Seabra, M. C.** 1998. Membrane association and targeting of prenylated Ras-like GTPases. Cell Signal. **10:**167–172.
27. **Wedlich-Soldner, R., S. Altschuler, L. Wu, and R. Li.** 2003. Spontaneous cell polarization through actomyosin-based delivery of the Cdc42 GTPase. Science **299:**1231–1235.
28. **Wu, H., G. Rossi, and P. Brennwald.** 2008. The ghost in the machine: small GTPases as spatial regulators of exocytosis. Trends Cell Biol. **18:**397–404.
29. **Wu, H., C. Turner, J. Gardner, B. Temple, and P. Brennwald.** 2010. The exo70 subunit of the exocyst is an effector for both cdc42 and rho3 function in polarized exocytosis. Mol. Biol. Cell **21:**430–442.
30. **Yakir-Tamang, L., and J. E. Gerst.** 2009. Phosphoinositides, exocytosis and polarity in yeast: all about actin? Trends Cell Biol. **19:**677–684.
31. **Yon, J., and M. Fried.** 1989. Precise gene fusion by PCR. Nucleic Acids Res. **17:**4895.
32. **Zhang, X., E. Bi, P. Novick, L. Du, K. G. Kozminski, J. H. Lipschutz, and W. Guo.** 2001. Cdc42 interacts with the exocyst and regulates polarized secretion. J. Biol. Chem. **276:**46745–46750.